Spectral Fiber Feature Space Evaluation for Crime Scene Forensics
Traditional Feature Classification vs. BioHash Optimization

Christian Arndt[1], Jana Dittmann[1,2] and Claus Vielhauer[1,3]

[1]*Otto-von-Guericke University Magdeburg, Dept. of Computer Science, Research Group Multimedia and Security,*
PO box 4120, 39016 Magdeburg, Germany
[2]*University of Buckingham, Applied Computing Dept., Buckingham MK18 1EG, U.K.*
[3]*Brandenburg University of Applied Sciences, Informatics and Media Dept., PO box 2132, 14737 Brandenburg, Germany*

Keywords: Digitized Crime Scene Forensics, Fiber Analysis, Identification, Individualization, Feature Space Evaluation.

Abstract: Despite of ongoing improvements in the field of digitized crime scene forensics, a lot of analysis work is still done manually by trained experts. In this paper, we derive and define a 2048 dimensional fiber feature space from a spectral scan with a wavelength range of 163 - 844 nm sampled with FRT thin film reflectometer (FTR). Furthermore, we perform an evaluation of seven commonly used classifiers (Naive Bayes, SMO, IBk, Bagging, Rotation Forest, JRip, J48) in combination with a proven concept from the biometric field of user authentication called Biometric Hash algorithm (BioHash). We perform our evaluation in two well-known forensic examination goals: identification - determining the broad fiber group (e.g. acrylic) and individualization - finding the concrete textile originator. Our experimental test set considers 50 different fibers, each sampled in four scan resolutions of: 100, 50, 20, 10 μm. Overall, 800 digital samples are measured. For both examination goals we can show that despite the Naive Bayes all classifiers show a positive classification tendency (80 - 99%), whereby the BioHash optimization performs best for individualization tasks.

1 INTRODUCTION

Alongside classic biometric traits such as fingerprints and face other trace types also play an important role in forensic crime scene investigations, such as textile fiber traces as a subcategory of micro traces. Nowadays, in the field of forensic fiber analysis, a trained expert's work is time-consuming and cost-intensive. Analysis work is often performed manually with only limited computing science support (SWGMAT, 1999; Houck and Siegel, 2010). Subjective expert's observations/decisions can be supported/strengthened by non-destructive and reproducible machine estimation.

Fibers indwell a high evidential value for various reasons. Besides their appearance in numerous high-profile cases, they rank among the frequently encountered physical evidence (Houck and Siegel, 2010). Since textiles and clothes are ubiquitous, fibers can potentially occur everywhere, even on crime scenes. One fundamental rule therefore is Locard's exchange principle - "Every contact leaves a trace". This quote states that no one can act/commit a crime with force/intensity without leaving numerous signs/marks (Inman and Rudin, 2001).

Apart from typical physical fiber characteristics - like diameter, delustrant, (reduces the sheen of chemical fibers), cross-sectional shape and morphological surface structure - fiber color also plays an important role. Although fiber color is one of the most distinguishing fiber characteristics (SWGMAT, 1999), it is also one of the most underutilized traits (Houck and Siegel, 2010). Hence, color should be analyzed spectrally and/or chemically. Therefore, we use a FRT thin film reflectometer (FTR) in our feature evaluation approach to cover both requirements. In respect to prior work, for a contactless and non-destructive data acquisition a chromatic white light sensor (CWL) (Hildebrandt et al., 2012) and a confocal laser scanning microscope (CLSM) (Arndt et al., 2012) were already evaluated regarding their technical suitability. Besides new opportunities in optical and spectral sensing, computing science offer several signal and pattern recognition techniques to support experts and derive result indications. Prior work has shown a positive result tendency regarding a computer-aided fiber identification - determining the broad fiber category - using supervised learning (Hildebrandt et al., 2012) as well as template matching (Arndt et al., 2012).

Therefore, we consider both matching methodologies in our experiments. Seven different supervised classifiers in a 2048 dimensional feature space and a template matching approach derived from the Biometric Hash algorithm (BioHash), introduced in biometrics (Vielhauer, 2006), are evaluated. By applying the known BioHash algorithm from the biometric field of dynamic handwriting, we want to compensate the intra-class variability of our spectral measurement data. Finally, we want to evaluate typical classifiers regarding their performance and the optimization impact of the BioHash algorithm within the feature space of 2048 spectral features from FTR sensing. We prepare, measure and evaluate 50 different fibers in four acquisition resolutions of: 100, 50, 20, 10 μm in our experiments. In summary, 400 scan samples are used for training and classification. Based on forensic case work, we consider two test goals: *identification* - determining the broad fiber category out of 5 different groups (e.g. acrylic) and *individualization* - finding the concrete textile originator out of 25 specific fiber types. In summary, we pursue three test objectives: **O1** for identification, **O2** for individualization and **O3** for comparing both aforementioned objectives by their achieved results.

This paper is structured as follows: In 2 we summarize the relevant state of the art and related work. The conceptual basis of our approach is introduced in 3. A detailed description of our experimental test setup is given in 4. Hereafter, obtained results are presented. Finally, we summarize our findings and derive future tasks in 6.

2 STATE OF THE ART

This section gives an overview of related research work in the field of forensic fiber analysis, relevant biometric topics and the used sensing device.

2.1 Forensic Fiber Analysis

Houck and Siegel define a textile fiber as a "unit of matter, either natural or manufactured, that forms the basic element of fabrics and other textiles [...]". This definition also describes the two main fiber categories: *natural* - a fiber, which exists in a natural state (e.g. plant fiber - cotton or animal hair - wool), *chemical* - derived from any substance by a process of manufacture (e.g. synthetic polymer - acrylic) (Houck and Siegel, 2010). Common forensic trace work starts with the physical trace acquisition on a crime scene. Every process step hereafter is done under laboratory conditions. Nowadays, textile fibers are typically

analyzed in a manual manor by trained experts with the help of special microscopes (SWGMAT, 1999). Achieved results are based on subjective expert decisions and often hard to comprehend and reproduce.

In a first examination step called *identification* (one-to-many comparison), a fiber trace is tentatively assigned to a broad group (e.g. natural or chemical fibers) based on characteristic optical features (e.g. surface characteristics), in order to limit the number of potential garments for individualization. *Individualization* on the contrary is perceived as the ultimate goal in forensic examination and it is denoted by a one-to-one comparison, searching for the textile origin (Inman and Rudin, 2001).

2.2 Related Work

Different spectrography-based research approaches in the context of textile fiber identification and individualization were already presented. Standard test methods encourage the usage of absorption spectra to distinguish between chemical fibers (AST, 2000). Stoeffler et al. (Stoeffler, 1996) introduced a flowchart system for the identification (nine generic classes) of synthetic fibers by transmissive polarized light microscopy. Another nondestructive approach presented by Prange et al. (Prange et al., 1995) based on total refection x-ray fluorescence (TXRF) uses characteristic trace element pattern for fiber identification. With the help of these "fiber fingerprints" 23 out of 35 samples (test-set contains: polyester, wool and viscose) were correctly assigned. Another differentiation technique using terahertz (THz) transmittance spectroscopy is introduced by Kurabayashi et al. (Kurabayashi et al., 2010). A three-dimensional excitation-emission matrix as feature space is utilized by Appalaneni et al. for the comparison of single fiber dyes (Appalaneni et al., 2014). Millington (Millington, 2012) uses UV-visible diffuse reflectance spectroscopy to analyze the color of undyed fibrous materials in the CIE XYZ color space. Nowadays Fourier transform infrared spectroscopy (FTIR) is the preferred method to determine fiber material properties (Houck and Siegel, 2010).

The FRT FTR thin film reflectometer (Fries Research & Technology GmbH (FRT), 2010) was already evaluated regarding the visibility assessment of latent fingerprints on challenging surfaces (Hildebrandt et al., 2013). This briefly summarized related work shows that several fiber identification approaches were successfully using either transmissive or reflectance spectrography-based sensing techniques.

A lot of research has been done so far in the field

of fiber identification, whereas the individualization gets only scarce attention. The German state police in Saxony-Anhalt and Berlin measure also the fiber absorption by transmittance-based FTIR techniques (UV-VIS wavelength range) for the purpose of fiber individualization.

2.3 Biometric Hash Algorithm

First test scans showed fluctuations within the fiber reflectance spectra of the same sample, similar to natural variations of biometric traits. The observation leads to the assumption that our feature space needs to be optimized regarding the intra-class variability of a sample, whilst preserving its discriminatory power. This is where the following algorithm comes into play.

The Biometric Hash algorithm (hereafter Bio-Hash), introduced by Vielhauer et al. (Vielhauer et al., 2002), is intentionally designed for online authentication in the field of dynamic biometric handwriting recognition. It is based on the idea of extracting a specific number of statistical features from a biometric raw signal that possesses a high intra-class variability. As a result of the BioHash generation the features are projected into a more stable representation, which minimizes the intra-class variability (fluctuations of feature manifestations of the same originator). The approach considers a transformation of every newly acquired biometric data sample into the BioHash feature space representation by means of special helper data. This helper data is called Interval Matrix *IM*, consisting of two vectors containing mapping interval lengths and offsets for each feature. During an enrollment process (training phase of a biometric system) to compensate the natural variability of handwriting, this particular IM generation is performed. Moreover, it is necessary to parameterize the BioHash generation by scaling the mapping intervals with the help of: Tolerance Vector *TV* - local impact of intra-class, individual feature variability and global Tolerance Factor *TF* - controls the tolerance of feature variability above the entire feature set. A more detailed description is given in (Vielhauer, 2006).

3 CONCEPT

In this section we propose our concept to address the identified research challenge.

Basically, our idea is to combine spectral measurement results of the FTR sensor with the Biometric Hash algorithm as matching methodology in order to minimize the intra-class variability. Our overall aim is

to classify textile fibers correctly based on their digital measurement data in both forensic use case scenarios - identification and individualization (see following 3.1 for pursued objectives). Besides this, the FTR sensor is evaluated regarding the suitability for digital fiber data acquisition. The discriminatory power of acquired spectral fiber measurement data is investigated as well.

To evaluate the FTR sampled 2048 dimensional feature space consisting of raw spectral data, as well as BioHash results, we suggest to use common pattern recognition pipelines as known e.g. from Jain (Jain, 1989), Vielhauer (Vielhauer, 2006) (see 1).
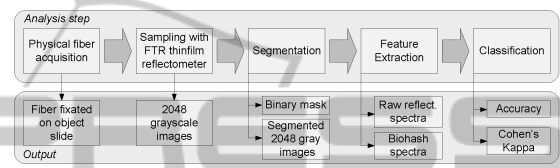

Figure 1: Fiber analysis pipeline for spectral classification.

3.1 Pursued Objectives

We derive our addressed objectives in relation to the well-known forensic uses cases (see 2).

O1 - Identification Assign the currently analyzed fiber to the correct broad category based on:

    O1.1 - raw, unaltered spectral data

    O1.2 - BioHash spectral data

O2 - Individualization Assign the currently analyzed fiber to the correct textile origin based on:

    O2.1 - raw, unaltered spectral data

    O2.2 - BioHash spectral data

O3 - Classification evaluation Compare both feature spaces by calculating the difference between raw and BioHash classifier performance:

    O3.1 - for *O1* identification

    O3.2 - for *O2* individualization

As quality measures for objective *O1* and *O2* the classifier prediction performance is evaluated using accuracy and Cohen's Kappa coefficient. Accuracy (correct classification rate in percent) is calculated by the number of correct assignments divided by the total of the population (0% - only false assignments, 100% - only correct assignments). The agreement between predicted and observed categorizations is measured by Kappa statistics (1 - 100% complete agreement, 0 - guess, negative values - beyond guessing) (Hall et al., 2009). The potential BioHash performance

boost is measured for *O3* by calculating the difference between BioHash and raw classification results in percent.

3.2 Proposed Analysis Pipeline

All utilized **physical specimen** are extracted either from labelled used clothes or new fiber threads with information about the origin. Different colors are chosen on purpose to consider this important characteristic. The test set, consisting of new and worn fibers, should clarify the question about the individualization ability - Can new fibers without individualization characteristics be individualized as well? Consequently, our test **objective** here is to group fibers of the same broad group (identification - *O1*) and concrete type (individualization - *O2*) with the help of spectral measurement results. Our matching methodology for *O1* is based on: five different classes - acrylic, polyester (chemical); alpaca, sheep wool (natural, animal hair); cotton (natural, plant origin) and for *O2*: 25 different textile donors - 25 individual classes (see 8 in the appendix).

Our test data is acquired with a spectroscopic **sensing device**, introduced in 3.3. On the contrary to common spectroscopic approaches, this sensor operates reflectively not transmissively. This device measures the reflectance energy in a particular spectral range. To ensure comparability between the FTR sensor data and measurement results of a confocal laser scanning microscope, a scan area of 675×506 *μm* is chosen, this corresponds to 20x magnification. In order to evaluate the suitability of this sensor, four different scan resolutions are measured for each specimen.

The process of **segmentation** is denoted by the separation of foreground fiber areas (relevant pixels in intensity images) and background underlying glass object slides. Our applied concept of Biometric Hashing requires a constant feature vector dimensionality and an equally distributed number of references for helper data creation (IM calculation) and hashing (BioHash feature generation). Therefore, it is necessary to determine which and how many segmented fiber pixels have to be considered for feature extraction. We consider both requirements by:

  i) determining the scan with the smallest spatial fiber expansion for each scan resolution,

  ii) binarizing this scan and count the number of foreground (white) fiber pixels and

  iii) selecting the beforehand determined fixed number of pixels for all fiber areas of this particular scan resolution.

The highest reflected spectral energy at 280 *nm* wave-

length, respectively the brightest foreground fiber gray-level intensity is the decisive criterion for the applied binarization with a global threshold. The following fixed numbers of selected fiber pixels are determined as appropriate for each lateral scan resolution (must be divisible by two): 100 *μm* - 8 px, 50 *μm* - 14 px, 20 *μm* - 68 px, 10 *μm* - 340 px.

Our proposed **feature space** consisting of a vector with 2048 dimensions per selected pixel is evaluated for both classification objectives (*O1*, *O2*). In detail, 2048 16-bit encoded integer values (range: 0 - 65535) are sampled per measured spot (selected fiber pixel in acquired data) and stored as raw reflectance spectra values with a wavelength range between 163 - 844 nm in steps of approx. 0.33 nm. These values can be considered as gray-level intensities and displayed as images, each per measured wavelength. To show the optimization capability of the BioHash algorithm, these feature vector representations are compared to raw, unaltered measurement results (*O3*).

In previous publications the following supervised learners achieved a satisfying **classification** performance. Furthermore, eager as well as lazy learning turned out to be suitable for the purpose of fiber identification. Nevertheless, their individualization suitability needs to be evaluated.

The following paragraph introduces all utilized supervised learners. *Naive Bayes* is a representative of simple probabilistic **classifiers** based on applying Bases' rules with strong (naive) independence assumptions. Support vector machines (SVM) select a small amount of critical boundary instances (called support vectors) and build a linear function for class separation (Witten et al., 2011). *SMO* (sequential minimal optimization) is an algorithm for SVM training and solves the quadratic programming optimization problem (Platt, 1998). *IBk*: Instance-based classification is denoted by a matching of one new instance against labelled and memorized instances in order to find the one which resembles it the most. The instance comparison is realized with a distance metric and neighborhood relation ($k = 1$ neighbor, Euclidean distance). This is called nearest neighbor classification (KNN). Meta or ensemble classifiers utilize multiple learning algorithms in order to achieve a better predictive performance. *Bagging* (bootstrap aggregating) derives one overall prediction out of various single decisions with equal weight. *Rotation Forest* on the contrary creates an ensemble of decision trees by combining bagging and random subspace approaches with principal component feature generation. *JRip* implements Weka's version of a propositional rule learner - Repeated Incremental Pruning to Produce Error Reduction (RIPPER). *J48* describes a

C4.5 (revision 8) decision tree learner developed by Ross Quinlan, which is an extension to the ID3 algorithm (Witten et al., 2011).

Every classifier that has been introduced so far is evaluated with a focus on the **predictive performance** in our two objectives *O1* and *O2*. In addition to that, these achieved classification results, based on raw and BioHash spectral feature data, are compared afterwards and assessed in relation to the BioHash improvement capabilities (*O3*).

3.3 Sensing

As a sensor device a broadband spectroscope is utilized in order to digitize our fiber samples. The FRT thin film reflectometer (FTR) was originally developed for thickness measurement of transparent films. A broadband light source (wavelength range: 163 - 844 nm) illuminates the specimen. As result of the interference of reflected light on the upper and lower boundary of the illuminated film a characteristic wavy pattern is measured. This characteristic wavy pattern in the reflectance spectra is denoted by layer thickness/wavelength ratio (Fries Research & Technology GmbH (FRT), 2010). Two separate optical fibers - illumination and detection - are joined in a single branch above the underlying specimen.

Our idea aims at deriving characteristic material properties, such as chemical composition and specific fiber color, from the fiber reflectance spectra. The technical suitability of this sensor device for the purpose of fiber identification and individualization is evaluated as well. Each physical specimen is sampled in four different scan resolutions with a point distance of: 100 μm, 50 μm, 20 μm and 10 μm (see 2). These chosen scan parameters seem to be a good compromise between scan duration and the necessary degree of detail for fiber data acquisition.

4 EXPERIMENTAL SETUP

Our experimental **test set** consists of 15 different worn clothes (individualization characteristics - way of usage, wearing and washing behavior) and 10 new fiber threads. Two fibers are extracted per donor (50 specimens) and prepared microscopically on glass object slides analogously to common forensic trace practice. An optimal scan specimen is denoted by a flat and planar lying fiber on the surface. In order to realize these conditions, the fiber is taped at both ends on the object slide. During the fiber extraction and preparation process the scan area (area between the taped fiber ends) is not exposed to any mechanical

(a) AWS1 100 μm at 280nm   (b) AWS1 50 μm at 280nm

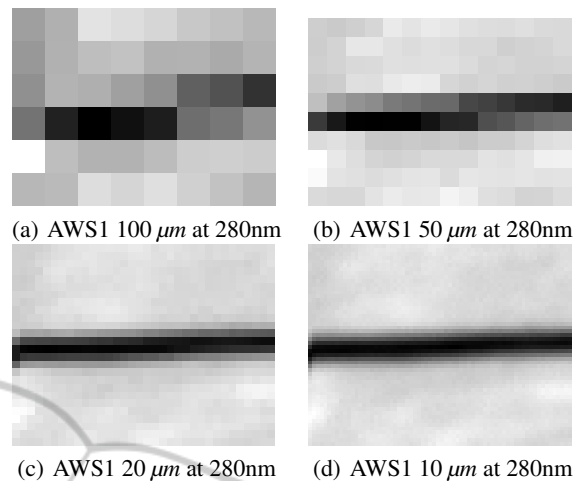(c) AWS1 20 μm at 280nm   (d) AWS1 10 μm at 280nm

Figure 2: Exemplary illustration: Four different scan resolutions of black alpaca wool AWS1 at 280 nm.

impact (e.g. squeeze them with tweezers). A complete overview of the used fibers, originating donors and considered types can be found in the appendix in 8.

Overall, 50 physical fiber specimen are microscopically prepared (5 broad groups $\times$ 5 representatives each $\times$ 2 samples per representative). Altogether 16 scans are digitized for each physical sample (2 consecutive scans $\times$ 2 measurement areas $\times$ 4 scan resolutions). Summarizing, 800 **measurement results** are sensed, whereas only 400 are part of our experimental test set. Consecutive scans are not considered in this work.

Every **sensor** scan is parameterized with an integration time of 150 ms (illumination duration) and the measurement head is adjusted manually on the z-axis (approx. 1 mm height above the specimen). The measured reflectance spectra is stored 16-bit encoded [0-65535] for each pixel in the respective scan resolution. Per pixel 2048 spectral values are measured between 163 nm and 844 nm in steps of approx. 0.33 nm. Depending on the beforehand adjusted lateral scan resolution, a finer, larger measurement result is obtained (scan duration increases as well). Point distances < 100 μm represent an oversampling due to the size of the illuminated spot.

The analysis steps of segmentation, feature extraction and BioHash generation are performed by a scientific software called "SpectroAnalyzer" (see 3), written in C# (.Net Framework version 4.5).

Image **segmentation** is realized by applying a manually selected global threshold to a gray-scale image. Spectral images at 280 nm offer a good contrast for binarization (see Figure 4(a)). Impurities like dust or other scan artifacts can be (de)-selected pixel-wise. As result a binary mask is created and stored for each
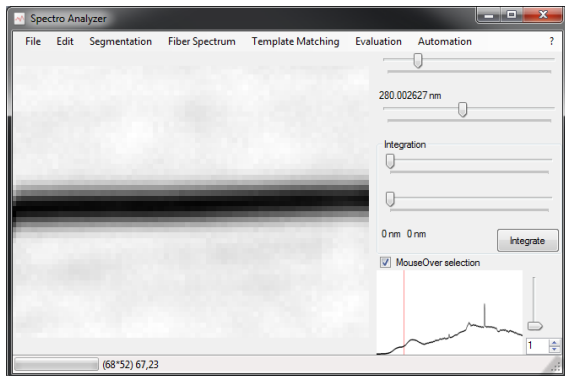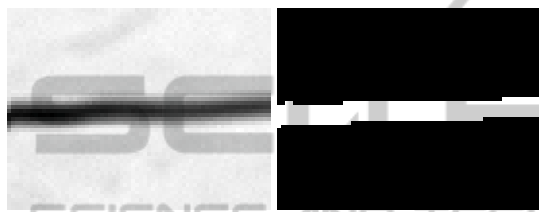
Figure 3: Screenshot of scientific software "SpectroAnalyzer", file opened: 10 μm scan of black alpaca wool ACB1

(a) Raw ACG1 at 280nm   (b) Segmented ACG1

Figure 4: Visualization: Segmentation process of gray acrylic fiber ACG1 at 280nm.

sample (see Figure 4(b)).

As already stated in 3.2, our segmentation approach consists of a selection of a fixed number of pixels (for each scan resolution), representing the maximum energy responses of the segmented fiber area. Neither pre-processing, nor feature normalization techniques are applied. Every segmented pixel and the corresponding **feature vector** is utilized for classification for both objectives *O1.1* and *O2.1*.

Objective *O1.2* and *O2.2* require the calculation of an interval matrix as helper data as well as the generation of BioHash vectors as actual features. Both are generated based on mutually exclusive data of equal size. Thus, this BioHash feature extraction procedure for *O1.2* and *O2.2* take place as follows:

Selected pixels of a sample are split into two equally sized and fully disjoint subsets by using even pixels and their corresponding feature vectors for IM calculation and odd ones for BioHash generation. Consequently, one half of the selected pixels is contributing to the IM calculation and the other half results in BioHash feature vectors. Thus, we calculate 4 BioHash feature vectors for a scan resolution of 100 μm and 7, 34, 170 vectors for 50 μm, 20 μm, 10 μm, respectively.

For any further steps the helper data (IM) is discarded and only resulting BioHash feature vectors are considered for training and classification. Standard

parameterization without local or global interval influence is applied for each $TV = 0$ and $TF = 1$

Our **classification** basis is also depending on four different scan resolutions and feature vectors, which are related to the number of segmented pixels (see 1). However, every feature space consists of 2048 spectral values, so 2048 attributes form our classification foundation. The number of classification instances is calculated by multiplying the segmented amount of fiber pixel with 100 (50 specimens $\times$ 2 measurement areas).

Table 1: Description of our classification basis.

Scan Property		No. Instances	
Resolution	No. Pixel	O1.1/O2.1	O1.2/O2.2
100 μm	8 px	800	400
50 μm	14 px	1400	700
20 μm	68 px	6800	3400
10 μm	340 px	34000	17000

Labelled raw and BioHash feature vectors are classified using Weka machine learning software (version 3.6.8) (Hall et al., 2009). Accuracy and Cohen's Kappa are used as quality measure for the classifier performance. Due to the limited amount of test-data a tenfold cross validation is applied for testing.

5 RESULTS

All obtained classification results are generated using Weka (version 3.6.8) (Hall et al., 2009) and rounded to two digits of precision. Bold printed values display the best classifier performance in the respective scan resolution. Classification results are presented in tabular form as follows: correct (cor.), incorrect (incor.) classified (accuracy), Cohen's Kappa (Kap.).

5.1 O1 - Identification

A fiber is assigned to the corresponding broad group (one out of five) based on *O1.1* raw spectral (see 2) and *O1.2* BioHash data (see 3). *O1.1*: As the scan resolution gets finer the accuracy increases as well. Rotation Forest achieved the best performance with one exception at 50 μm. *O1.2*: The BioHash seems to improve the overall classification performance, even on smaller resolutions. SMO and IBk achieve the best performance for this objective, whereas Naive Bayes shows the poorest.

Table 2: *O1.1* - Classification results of identification based on raw spectral data.

Classifier	100 μm			50 μm			20 μm			10 μm		
	cor.	incor.	Kap.	cor.	incor.	Kap.	cor.	incor.	Kap.	cor.	incor.	Kap.
N. Bayes	64.63	35.38	0.56	66.21	33.79	0.58	69.74	30.26	0.62	68.85	31.15	0.61
SMO	87.38	12.63	0.84	91.00	9.00	0.89	96.81	3.19	0.96	98.76	1.24	0.98
IBk	94.75	5.25	0.93	**96.79**	**3.21**	**0.96**	98.91	1.09	0.99	99.70	0.30	1.00
Bagging	82.75	17.25	0.78	88.14	11.86	0.85	93.96	6.04	0.92	96.99	3.01	0.96
R. Forest	**94.88**	**5.13**	**0.94**	96.50	3.50	0.96	**99.25**	**0.75**	**0.99**	**99.77**	**0.23**	**1.00**
JRip	77.50	22.50	0.72	83.71	16.29	0.80	90.88	9.12	0.89	95.48	4.52	0.94
J48	78.88	21.13	0.74	85.29	14.71	0.82	92.15	7.85	0.90	94.61	5.39	0.93

Table 3: *O1.2* - Optimized classification results of identification based on BioHash spectral data.

Classifier	100 μm			50 μm			20 μm			10 μm		
	cor.	incor.	Kap.	cor.	incor.	Kap.	cor.	incor.	Kap.	cor.	incor.	Kap.
N. Bayes	42.00	58.00	0.28	39.71	60.29	0.25	45.15	54.85	0.31	59.42	40.58	0.49
SMO	95.75	4.25	0.95	**99.71**	**0.29**	**1.00**	**99.82**	**0.18**	**1.00**	99.91	0.09	1.00
IBk	**99.50**	**0.50**	**0.99**	98.57	1.43	0.98	99.41	0.59	0.99	**99.94**	**0.06**	**1.00**
Bagging	97.00	3.00	0.96	98.57	1.43	0.98	98.97	1.03	0.99	99.58	0.42	0.99
R. Forest	99.25	0.75	0.99	99.43	0.57	0.99	99.62	0.38	1.00	99.92	0.08	1.00
JRip	89.25	10.75	0.87	94.00	6.00	0.93	98.12	1.88	0.98	99.53	0.47	0.99
J48	95.25	4.75	0.94	92.43	7.57	0.91	98.09	1.91	0.98	99.46	0.54	0.99

5.2 O2 - Individualization

O2.1: Our obtained individualization results resemble the identification ones (see 4 and 5). Nevertheless, at 100 μm in comparison to *O1* our results are a little bit worse. Yet, at this point it has to be noted that one out of 25 classes is assigned here. However, Rotation Forest and IBk perform well again. Rotation Forrest achieved the best overall performance of objective *O2.1* at 10 μm with 99.77% correct assigned fibers. For objective *O2.2*, the Bagging classifier was able to correctly assign every fiber at 50 μm. Besides this, IBk and SMO classify as satisfying as well, while Naive Bayes performs with low accuracy again.

5.3 O3 - Classification Evaluation

6 and 7 show the classifier performance difference between BioHash and raw feature data. Negative values point at a classification performance deterioration of the BioHash algorithm in comparison to raw spectral data. An average of all classifier results and Kappa values of the same column is presented in the last tabular line.

O3.1: as the resolution gets finer the BioHash performance improvement is decreased. Nonetheless, almost every classifier accuracy and Kappa is improved, except for the Naive Bayes. *O3.2*: In comparison to *O3.1* the average improvement of *O3.2* is significantly higher. The JRip classifier results are increased by remarkable 37.75% at 100 μm. Similar to *O3.1* the

BioHash improvement effect of classifiers with lower predictive performance is higher (e.g. Bagging, JRip, J48). On the contrary, the results of the Naive Bayes learner are getting worse, especially for *O3.1*.

6 CONCLUSION

We conclude our findings and derive future tasks in the following section. Our achieved results showed the optimization influence of the BioHash algorithm. Nevertheless, the impact is significantly higher at individualization tasks, which is reasonable because classification results based on raw spectral data are already very promising (around 90%). According to this, the Biometric Hash algorithm is capable of boosting almost every tested classifier's accuracy, without favoring false assignments. Better predicting classifiers in objective *O1.1* and *O2.1* are less influenced by the BioHash optimization effect and vice versa. For the purpose of identification the following classifiers performed satisfyingly on our test data: *O1.1* - IBk; Rotation Forrest; *O1.2* - SMO, IBk, Bagging, Rotation Forrest, J48. Whereas for individualization our best performing classifiers are: *O2.1* - SMO, IBk, Rotation Forrest; *O2.2* - SMO, IBk, Bagging, Rotation Forrest, J48.

It seems to be rather predictable that the overall performance of the Naive Bayes classifier is low in comparison to all the others. Unfortunately, the strong independence assumptions are not fulfilled by our fea-

Table 4: *O2.1* - Classification results of individualization based on raw spectral data.

Classifier	100 μm			50 μm			20 μm			10 μm		
	cor.	incor.	Kap.	cor.	incor.	Kap.	cor.	incor.	Kap.	cor.	incor.	Kap.
N. Bayes	52	48	0.5	52.79	47.21	0.51	53.28	46.72	0.51	49.65	50.35	0.48
SMO	87.75	12.25	0.87	94.00	6.00	0.94	97.44	2.56	0.97	98.19	1.81	0.98
IBk	82.13	17.88	0.81	88.43	11.57	0.88	95.91	4.09	0.96	**98.81**	**1.19**	**0.99**
Bagging	64.25	35.75	0.63	71.64	28.36	0.70	85.28	14.72	0.85	90.74	9.26	0.90
R. Forest	**91.13**	**8.88**	**0.91**	**94.21**	**5.79**	**0.94**	**97.79**	**2.21**	**0.98**	98.80	1.20	0.99
JRip	50.00	50.00	0.48	54.57	45.43	0.53	76.13	23.87	0.75	84.63	15.37	0.84
J48	60.75	39.25	0.59	66.93	33.07	0.66	78.56	21.44	0.78	83.31	16.69	0.83

Table 5: *O2.2* - Optimized classification results of individualization based on BioHash spectral data.

Classifier	100 μm			50 μm			20 μm			10 μm		
	cor.	incor.	Kap.	cor.	incor.	Kap.	cor.	incor.	Kap.	cor.	incor.	Kap.
N. Bayes	61.50	38.50	0.60	48.00	52.00	0.46	56.85	43.15	0.55	60.21	39.79	0.59
SMO	95.00	5.00	0.95	99.57	0.43	1.00	**99.79**	**0.21**	**1.00**	99.87	0.13	1.00
IBk	**99.25**	**0.75**	**0.99**	98.43	1.57	0.98	99.21	0.79	0.99	**99.86**	**0.14**	**1.00**
Bagging	**99.25**	**0.75**	**0.99**	**100.00**	**0.00**	**1.00**	99.18	0.82	0.99	99.43	0.57	0.99
R. Forest	98.50	1.50	0.98	98.57	1.43	0.99	98.88	1.12	0.99	99.81	0.19	1.00
JRip	87.75	12.25	0.87	92.57	7.43	0.92	96.97	3.03	0.97	99.12	0.88	0.99
J48	93.00	7.00	0.93	90.00	10.00	0.90	97.18	2.82	0.97	99.04	0.96	0.99

Table 6: *O3.1* - Comparison of raw identification and optimized BioHash classification results.

Classifier	100 μm		50 μm		20 μm		10 μm	
	Cl. imp.	Ka. imp.	Cl. imp.	Ka. imp.	Cl. imp.	Ka. imp.	Cl. imp.	Ka. imp.
N. Bayes	-22.63	-0.28	-26.50	-0.33	-24.59	-0.31	-9.43	-0.12
SMO	8.38	0.10	8.71	0.11	3.01	0.04	1.16	0.01
IBk	4.75	0.06	1.79	0.02	0.50	0.01	0.24	0.00
Bagging	14.25	0.18	**10.43**	**0.13**	5.01	0.06	2.58	0.03
R. Forest	4.38	0.05	2.93	0.04	0.37	0.00	0.15	0.00
JRip	11.75	0.15	10.29	0.13	**7.24**	**0.09**	4.05	0.05
J48	**16.38**	**0.20**	7.14	0.09	5.94	0.07	**4.84**	**0.06**
Average	5.32	0.07	2.11	0.03	-0.36	0.00	0.51	0.01

Table 7: *O3.2* - Comparison of raw individualization and optimized BioHash classification results.

Classifier	100 μm		50 μm		20 μm		10 μm	
	Cl. imp.	Ka. imp.	Cl. imp.	Ka. imp.	Cl. imp.	Ka. imp.	Cl. imp.	Ka. imp.
Naive Bayes	9.50	0.10	-4.79	-0.05	3.57	0.04	10.56	0.11
SMO	7.25	0.08	5.57	0.06	2.35	0.02	1.68	0.02
IBk	17.13	0.18	10.00	0.10	3.29	0.03	1.05	0.01
Bagging	35.00	0.36	**28.36**	**0.30**	13.90	0.14	8.69	0.09
Rot. Forest	7.38	0.08	4.36	0.05	1.09	0.01	1.01	0.01
JRip	**37.75**	**0.39**	38.00	0.40	**20.84**	**0.22**	14.49	0.15
J48	32.25	0.34	23.07	0.24	18.62	0.19	**15.73**	**0.16**
Average	20.89	0.22	14.94	0.16	9.09	0.09	7.60	0.08

ture vectors. Thus, applying the BioHash on objective *O1.2* makes it even worse. The individualization results *O2.2* for this classifier are not affected negatively in such a degree. Highly sophisticated classifiers like Bagging, Rotation Forrest or SMO perform well on the one hand, but a lazy learner like IBk, achieves very

good results on the other hand, too. Nevertheless, when it comes to computational effort, the k-nearest neighbor approach of the IBk, with model generation and evaluation at the same time, is in front. However, IBk behaves better on the BioHash optimized feature space. Thus, a resemblance to the BioHash as a tem-

plate matching approach can be seen since it also uses a nearest neighbor algorithm.

Furthermore, the FRT sensor is evaluated regarding the suitability for fiber trace acquisition. Scans with 100 μm resolution are affected the most by the BioHash optimization capabilities. Nonetheless, classification results, generated from more detailed scans, are also improved by applying our BioHash methodology. However, we recommend scans with a point distance smaller than 100 μm (100 μm suitable for coarse scan, e.g. fiber detection), even though it is an oversampling with the utilized device. Although, new and worn fibers can be assigned correctly by our introduced analysis pipeline, it is not clarified if the chemical composition or color is the distinguishing characteristic expressed in our analyzed measurement data. So the question concerning an individualization without particular characteristics cannot be answered conclusively.

6.1 Limitations

Some decisions that were made are accompanied by limitations. Regarding our test data acquisition, the working distance between measurement head and specimen is adjusted manually. Due to the time-consuming acquisition procedure (between 10s - 100 μm and 20 min - 10 μm scan) only a limited amount of test data is evaluated. Concerning the Bio-Hash algorithm, no parameterization for the interval mapping is evaluated. Neither a tolerance factor nor a tolerance vector was empirically pre-determined (both set to default values). Only default parameter settings for all classifiers as well as for the Bio-Hash are used in our tests. Our evaluated spectral feature space is not yet analyzed in respect to the expressed fiber characteristics in our obtained measurement data. Therefore, it needs to be investigated which physical fiber characteristic (chemical or color property) is measured and thereby represented in the spectral data. Nevertheless, our experimental methodology was chosen carefully to avoid such side effects. Furthermore, it could be crucial to analyze the chemical composition of fibers and their color in order to evaluate the discriminatory power of individualization characteristics.

6.2 Future Work

To strengthen our results that are shown in this paper a larger amount of experimental data needs to be evaluated with fully disjoint sets of training and test data for the purpose of classification. Besides this, different sensor parameterization should be evaluated re-

garding their influence on the classification accuracy (e.g. working distance, integration time). Will different scans of the exact same sample lead to the same classifier prediction? A feature selection could be performed on our large wavelength range feature space. Band-pass or -block filters can be applied in order to emphasize or ignore certain wavelengths (e.g. peaks, which express certain lamp characteristics). Furthermore, an optimization regarding a suitable BioHash tolerance factor and vector for the interval mapping could be potentially useful. A different way of a BioHash training phase for interval matrix generation should be designed in order to gain more data for the BioHash feature generation. To achieve a higher degree of measurement data reproduction-ability, other procedures of data acquisition should be considered. Our sampled consecutive scans can be assessed using a differential imaging approach. Finally, different spectroscopic sensors, with transmissively or reflectively working principle, should be comparatively evaluated with our physical specimens.

REFERENCES

(2000). Standard test methods for identification of fibers in textiles.

Appalaneni, K., Heider, E. C., Moore, A. F. T., and Campiglia, A. D. (2014). Single fiber identification with nondestructive excitation-emission spectral cluster analysis. *Analytical Chemistry*, 86(14):6774–6780. PMID: 24432828.

Arndt, C., Kraetzer, C., and Vielhauer, C. (2012). First approach for a computer-aided textile fiber type determination based on template matching using a 3d laser scanning microscope. In *Proceedings of the 14th workshop on Multimedia and Security*, MMSec '12, pages 57–66. ACM, New York, NY, USA.

Fries Research & Technology GmbH (FRT) (2010). Data sheet frt ftr - thin film reflectometer.

Hall, M., Frank, E., Holmes, G., Pfahringer, B., Reutemann, P., and Witten, I. H. (2009). The weka data mining software: An update. *SIGKDD Explor. Newsl.*, 11(1):10–18.

Hildebrandt, M., Arndt, C., Makrushin, A., and Dittmann, J. (2012). Computer-aided fiber analysis for crime scene forensics. In Bouman, C. A., Pollak, I., and Wolfe, P. J., editors, *Proc. of SPIE 8296, Computational Imaging X, 829601*, volume 8296.

Hildebrandt, M., Makrushin, A., Qian, K., and Dittmann, J. (2013). Visibility assessment of latent fingerprints on challenging substrates in spectroscopic scans. In De Decker, B., Dittmann, J., Kraetzer, C., and Vielhauer, C., editors, *Communications and Multimedia Security*, volume 8099 of *Lecture Notes in Computer Science*, pages 200–203. Springer Berlin Heidelberg.

Houck, M. M. and Siegel, J. A. (2010). *Fundamentals of Forensic Science*. Academic Press, 2nd edition edition.

Inman, K. and Rudin, N. (2001). *Principles and Practice of Criminalistics - The Profession of Forensic Science*. CRC Press.

Jain, A. K. (1989). *Fundamentals of Digital Image Processing*. Prentice Hall.

Kurabayashi, T., Saitoh, F., Watanabe, N., and Tanno, T. (2010). Identification of textile fiber by terahertz spectroscopy. In *Proc: 35th International Conference on Infrared Millimeter and Terahertz Waves (IRMMW-THz)*, pages 1–2.

Millington, K. R. (2012). Diffuse reflectance spectroscopy of fibrous proteins. *Amino Acids*, 43(3):1277–1285.

Platt, J. C. (1998). Sequential minimal optimization: A fast algorithm for training support vector machines. Technical report, Advances in Kernel Methods - Support Vector Learning.

Prange, A., Reus, U., Boeddeker, H., Fischer, R., and Adolf, F.-P. (1995). Microanalysis in forensic science: Characterization of single textile fibers by total reflection x-ray fluorescence. In *Analytical Sciences*, volume 11, pages 483–487.

Stoeffler, S. (1996). A flowchart system for the identification of common synthetic fibers by polarized light microscopy. *Journal of Forensic Sciences*, 41:297–299.

SWGMAT (1999). Forensic fiber examination guidelines. Online available: http://www.swgmat.org/Forensic %20Fiber%20Examination%20Guidelines.pdf.

Vielhauer, C. (2006). *Biometric User Authentication for IT Security - from Fundamentals to Handwriting*. Springer Science+Business Media, Inc.

Vielhauer, C., Steinmetz, R., and Mayerhofer, A. (2002). Biometric hash based on statistical features of online signatures. In *Pattern Recognition, 2002. Proceedings. 16th International Conference on*, volume 1, pages 123–126.

Witten, I. H., Frank, E., and Hall, M. A. (2011). *Data Mining Practical Machine Learning Tools and Techniques*. Elsevier, 3. auflage edition.

APPENDIX

Table 8: Experimental test-set description.

No.	Identifier	Fiber Type	Color	Donor
Natural Fibers: Animal Hair - Alpaca Wool				
1	AWB	alpaca wool	beige	new wool thread
2	AWBR	alpaca wool	brown	new wool thread
3	AWG	alpaca wool	green	new wool thread
4	AWS	alpaca wool	black	new wool thread
5	AWW	alpaca wool	white	new wool thread
Natural Fibers: Animal Hair - Sheep Wool				
6	SWB	sheep wool	beige	used sweater
7	SWG	sheep wool	gray	used sweater
8	SWO	sheep wool	olive-green	used sweater
9	SWR	sheep wool	red	used cardigan
10	SWS	sheep wool	black	used cardigan
Natural Fibers: Plant - Cotton				
11	BWW	cotton	white	used shorts
12	BWR	cotton	red	used shorts
13	BWK	cotton	khaki	used shirt
14	BWG	cotton	light gray	used shorts
15	BWS	cotton	black	used T-shirt
Chemical Fibers - Acrylic				
16	ACB	acrylic	blue	used knitted cap
17	ACG	acrylic	gray	used knitted cap
18	ACDG	acrylic	dark gray	used knitted cap
19	ACS	acrylic	black	used cap
20	ACW	acrylic	white	used cap
Chemical Fibers - Polyester				
21	PEB	polyester	blue	new sewing thread
22	PEG	Polyester	yellow	new sewing thread
23	PER	Polyester	red	new sewing thread
24	PES	Polyester	black	new sewing thread
25	PEW	Polyester	white	new sewing thread